IEEE Access
Multidisciplinary | Rapid Review | Open Access Journal

Date of publication xxxx 00, 0000, date of current version xxxx 00, 0000.

Digital Object Identifier 10.1109/ACCESS.2017.Doi Number

Hierarchical Control Implementation for Meshed AC/Multi-terminal DC Grids with Offshore Windfarms Integration

F. Akhter[1], S. S. H. Bukhari[1], F. H. Mangi[1], D. E. Macpherson[2], G. P. Harrison[2], W. Buhksh[3] and J. S. Ro[4]

[1]Department of Electrical Engineering, Sukkur IBA University, airport road, Sukkur 65200, Pakistan
[2]School of Engineering, University of Edinburgh, Edinburgh, UK
[3]Department of Electronic and Electrical Engineering, University of Strathclyde, Glasgow, UK
[4]School of Electrical and Electronics Engineering, Chung-Ang University, Seoul, South Korea

Corresponding author: Jong-Suk Ro (e-mail: jongsukro@gmail.com).

This research was supported in part by the National Research Foundation of Korea funded by the Ministry of Education (2016R1D1A1B01008058), Korea Electric Power Corporation (Grant number:R17XA05-30), and by Korea Research Fellowship Program through the National Research Foundation (NRF) of Korea funded by the Ministry of Science and ICT (2019H1D3A1A01102988).

ABSTRACT Although the integration of meshed multi-terminal direct current (MTDC) grids with the existing AC grid has some added economic advantages, significant challenges are encountered in such systems. One of the major challenges is ensuring secure and optimal operation of the combined AC/MTDC grid considering the stability requirements of AC and DC grids at different operating conditions. This paper presents the implementation of hierarchical control for the combined AC/MTDC grid. The hierarchical control is based on the well-established three-layered control of the AC power system, comprising primary, secondary, and tertiary controls. A set of appropriate control methods are proposed for the primary, secondary, and tertiary control layers to accomplish the identified requirements for secure and optimal operation of the combined AC/MTDC grid.

INDEX TERMS AC multi-terminal direct current grid, droop control, optimized operation, power flow control

I. INTRODUCTION

Electricity generation from offshore wind farms is one of the most favorable sources to meet the growing global energy demand. In recent years, the penetration of offshore wind energy has significantly increased. To exploit the enormous potential of wind energy, more offshore wind farms (OWFs) are scheduled to be connected in the North Sea by 2030 [1].

However, there are many challenges to be addressed in order to harness offshore wind energy resources. One of the main challenges is the transmission of power from remote OWFs to onshore demand centers. Another challenge is balancing supply and demand in the power system owing to the large variability of power from OWFs. A meshed grid structure through efficient sharing of offshore wind energy resources is considered an attractive option for reliable operation of the system owing to the expected increase in the number of offshore installations [2].

The behavior of a multi-terminal direct current (MTDC) grid is different from that of a conventional AC grid mainly because of the use of fast-acting power electronics devices in an MTDC grid. Moreover, given the general inexperience in dealing with MTDC grids, the integration of MTDC grids with the traditional AC grid introduces new operational and controllability challenges for the combined system. In this context, appropriate and detailed models are required to determine the operation of the combined grid. The steady state interaction between the AC grid and MTDC grid has not been elucidated; thus, the following areas should be investigated:

- How will the combined AC/MTDC system behave under various operating conditions?
- What is the best operating strategy for power flow control in the combined AC/MTDC system?

Previous studies on MTDC grid mainly focused on the control dynamics of the grid without considering the

This article has been accepted for publication in a future issue of this journal, but has not been fully edited. Content may change prior to final publication. Citation information: DOI 10.1109/ACCESS.2019.2944718, IEEE Access

behavior of the AC grid. Several control configurations have been previously proposed [3]–[14]; most of the configurations focused on different modifications of the droop control. Furthermore, several studies have proposed power flow solutions for the MTDC grid without considering MTDC control configurations [15]–[19]. Some studies have also carried out detailed modelling of the combined AC/DC systems [20]–[25]. However, in these studies, the control configurations were either not taken into account or only a specific control configuration was considered. The study in [26] addressed the problem of non-linear droop implementation in MTDC grid power flows and proposed a method to use the mean voltage instead of the voltage of a single slack bus in the MTDC grid while the AC/DC grids were solved separately.

Two core methods can be employed for the combined AC/MTDC power flow (C-PF) calculations, namely sequential and unified methods. The study in [27] demonstrated a sequential power flow approach with a complete model of the MTDC system. Losses due to the coupling transformer, filters, and converter were included in the power flow calculations. The unified power flow approach uses the modified Jacobian technique [21][26], in which the power flow calculation is performed by solving the integrated AC/MTDC scheme simultaneously and all the variables are accessible after subsequent iterations. In the sequential method, by contrast, the AC/MTDC scheme is solved sequentially (one by one) [20], although the work primarily focused on embedded MTDC grid in AC grids. The study in [28] proposed a multi-option power flow technique in which an MTDC system connected to a number of asynchronous AC networks was solved. However, DC voltage droop controls were not incorporated while modelling the voltage source converter (VSC) stations. The implementation of a DC power flow algorithm with generic droop lines using a method that specifies the mean voltage instead of a single slack bus in the MTDC grid was proposed in [26]. This results in the problem of solving more than one AC or DC grid in the C-PF algorithm because the MTDC grid is expected to interconnect large AC grids. More variables should be included for a combined solution of an AC/DC scheme having multiple AC and DC grids.

Several studies extended the optimal power flow problem to optimize the operation of the combined AC/MTDC grid [29]–[34]. A few studies [26]–[27] focused on the security constraints for combined optimization with a set of linearized power flow equations to avoid computation complexity. However, a linearized power flow equation may not yield accurate settings for voltage and reactive power on the AC side of the system. To address this, this study uses nonlinear AC power flow equations to model the AC side. The resulting optimal solution was evaluated for a given security criterion. If the solution does not meet the security criterion, decision-based corrective control is implemented.

The core contributions of this paper are as follows:

- A new hierarchical framework is proposed for steady state control of AC/MTDC grids.
- A generic tri-band droop control is proposed for meshed AC/MTDC grids with OWF integration.
- A generalized C-PF algorithm is implemented, which performs generic droop control for a combined AC/MTDC grid.
- An iterative modelling framework that incorporates a security criterion and optimal power flow is implemented to determine the control parameters of an AC/MTDC grid.
- Application of the proposed framework on an extended 14-bus network is demonstrated.

The rest of the paper is organized as follows. In section 2, the proposed hierarchal control framework is described. Section 3 presents the generic tri-band droop control for primary regulation, whereas Section 4 presents the algorithm for combined power flow of secondary control. Section 5 describes the security constrained optimization for tertiary control to obtain a secured and optimal operation of combined AC/MTDC grids. Finally, the results of a test case are presented in Section 6, and the conclusions of the study are described in Section 7.

II. PROPOSED HIERARCHICAL CONTROL FRAMEWORK

A systematic control structure is required to operate a combined AC/MTDC grid. The main objective of a systemized control structure is to obtain the desired power flows from the MTDC grid, while maintaining a stable DC node voltage within the operating limits. In case of a disturbance or outage in an MTDC grid with more than one VSC station controlling the DC node voltage, the new operating point is determined by the VSC station with the lowest reference set point when under centralized control or according to the characteristics of the distributed control of the participating VSC stations. The hierarchical control structure of the MTDC grid can be divided into high and low levels, as shown in Fig. 1. High level control comprises primary, secondary, and tertiary controls, similar to an AC system [37]–[41], whereas low level control comprises the basic inner current and firing control of the VSC stations. The inner controller of the VSC station can be implemented by two different methods, direct control and vector (d-q decoupled) control. In the case of direct control, the voltage magnitude and phase angle are directly controlled by adjusting the modulation index m and phase shift δ respectively, in response to the comparison of the controlled parameters with the reference parameters. The direct voltage control requires the voltage and current phasor measurements from the point of common coupling (PCC). Whereas in vector control, also known as d-q decoupled control, the active and reactive power can be controlled independently by using the d-q current control strategy which can inherently limit the overloading of switches. The control configuration

This article has been accepted for publication in a future issue of this journal, but has not been fully edited. Content may change prior to final publication. Citation information: DOI 10.1109/ACCESS.2019.2944718, IEEE Access

of the VSC station based on decoupled control comprises of cascaded control, with a faster inner controller and an outer controller to provide reference parameters to the inner controller. The outer control provides a reference for the d-axis current to control either active power or DC node voltage. It also provides a reference for q-axis current for controlling either reactive power or AC grid voltage depending on AC grid requirements.

The responsibility of managing the DC node voltage regulation can be regarded as primary control, similar to primary control in an AC system with frequency regulation. Secondary control can be implemented to adjust power exchanges from the MTDC grid to restore the pre-disturbance conditions in the grid. Tertiary control can be implemented to obtain the optimized reference set-points for primary and secondary controls.

The power–DC voltage characteristics of an MTDC grid are similar to the power–frequency characteristics of an AC system. However, frequency is a universal parameter in an AC system, whereas DC node voltage varies at each VSC station according to the actual power flow and voltage drop in the MTDC grid. Second, stored energy in the MTDC grid is very limited (to only capacitors and cables), compared to the kinetic energy in AC rotating machines. This makes the power–DC voltage characteristics more sensitive than the power–frequency characteristics of an AC system. Hence, the response of the controller in the MTDC grid is faster, resulting in smaller time constants for the high-level controls of the MTDC grids. The primary control of the MTDC grid is activated in a few milliseconds compared to a time constant of 10–15 s for the AC system's primary control. The secondary control activates in a few seconds, whereas the tertiary control reacts in tens of minutes to one hour.

However, despite these advantages, one challenge encountered in the meshed MTDC grid is power controllability. An appropriate systemized control structure is required to maintain the precise power flow through the meshed MTDC grid.

III. GENERIC TRI-BAND DROOP CONTROL (GTB DROOP) – PRIMARY CONTROL

Primary control is required to act automatically in response to power imbalance in the MTDC grid, without external communication. Some of the important requirements are given in [42], and are summarized below:

- Precise control under normal operation
- Stable operation under disturbance
- Automatic dynamic power sharing
- Overload prevention
- Operation within permitted limits
- Rescheduling capability.

Fast and direct response is required from the primary control. The DC voltage control methods implemented in the outer control loop of the VSC station are considered for primary control of the MTDC grid, similar to frequency droop control for the AC system, as shown in Fig. 1.

Distributed voltage control can be implemented in an MTDC grid by applying linear droop control to the VSC stations required to participate in DC voltage regulation; similar to the implementation of frequency droop control in an AC system. Distributed voltage control can provide a stable operating point during disturbances in a large MTDC grid. No single station is exposed to high stresses and oversizing is not required, unlike centralized voltage control, as the power fluctuations in the MTDC grid are distributed among several participating VSC stations. Further, a back-up mechanism is not required to provide N-1 security in distributed voltage control. Power sharing among the DC voltage regulating VSC stations is determined by the relative droop constant values of the VSC stations. The VSC station with the smallest droop constant value will have the highest share of the power and vice versa.

However, with implementation of simple linear droop control, the response time of the VSC station varies directly with the amount of disturbance, which may lead to unstable operation of the MTDC grid. Hence, appropriate primary control is required to regulate the response of the VSC stations in the stable operating region.

Further, under droop control, the new operating points following a disturbance do not track the reference set points and result in deviation from the desired power flow in the MTDC grid. Therefore, the establishment of a stable operating point and the desired power flow following an outage or disturbance requires appropriate secondary control for the MTDC grid.

In the case of active-band droop control, the response to disturbances is the same as the droop constants for the lower and upper bands are the same. However, power imbalances in the MTDC grid can be further distinguished as imbalance due to excessive (i.e. uncontrolled) injections from the OWF and power shortage due to outage of a major component.

Active-band control can be extended to have two different droop constants in the upper and lower bands in addition to normal band droop in order to add more flexibility for control of two different disturbances at the primary control level. This allows the operator to change the response for two different disturbances through secondary control. The implementation of the tri-band droop control is the same as the active-band droop, except for the difference in the values of the droop constant for the upper and lower bands, as shown in Fig. 2.

IV. POWER FLOW ALGORITHM FOR AC/MTDC GRIDS WITH GTB DROOP – SECONDARY CONTROL

Secondary control is required to achieve the desired power flow sharing between AC and DC grids following a disturbance in the AC/MTDC grid. It acts as coordination control among the VSC stations in the MTDC grid to provide updated power and DC voltage references. Secondary control

This article has been accepted for publication in a future issue of this journal, but has not been fully edited. Content may change prior to final publication. Citation information: DOI 10.1109/ACCESS.2019.2944718, IEEE Access

actions under coordinated control provide updated references that determine the overall steady state power flows in the MTDC grid to restore the voltages within the required profile and planned operation [42].

A centralized coordinated control system can be implemented as secondary control to communicate the updated settings of the VSC and generator units to maintain the desired power flows from both MTDC and AC grids, which may include the following:

- Power and DC voltage references (P_{REF} and V_{REF}) for each VSC station and AC generator unit;
- Droop gains for individual droop band (K_{DC1}, K_{DC2}, and K_{DC3}) of each VSC station;
- Band limits settings (i.e., $V_{DC\ HIGH}$ and $V_{DC\ LOW}$).

The centralized coordinating controller requires actual measurements from the remote terminal units (RTU) of all VSC stations to determine the actual operation of the MTDC grid. These include the actual converter power and DC node voltages with their limit settings such as the maximum and minimum DC voltage and power limits, including any individual-assigned band DC voltage limits for specific control configurations, such as voltage margin and tri-band droop control. The implementation of the coordinated control is shown in Fig. 2. The communication system used for coordinated control is assumed to be reliable. In the case of loss of communication, the operation will still be stable, but without the desired power flow sharing between AC and DC grids, as primary control is autonomous. Rescheduling from coordinated control can be set to event-based or cyclic in the time span of a few minutes.

A. COMBINED AC/MTDC POWER FLOW: PROBLEM STATEMENT

The C-PF provides a steady state operating point for integrated AC/MTDC grids. It can be used in secondary control for rescheduling power and voltage references of VSC stations, wind integration analysis, and N-1 security assessments. However, the power–voltage relations in a DC grid are not similar to those of an AC grid. The C-PF can be obtained by solving dissimilar sets of numerical equations. Fig. 3 shows the VSC model for AC/MTDC grid integration. The application of various DC voltage control modes of the VSC stations to the MTDC system increases the complexity.

The operational flexibility of distributed control makes it more advantageous, as the DC link voltage is controlled by multiple VSC stations of the MTDC system. It is essential to establish a comprehensive C-PF model of the MTDC grids along with large interconnected AC grids. This ensures that the steady state operating point is determined, which includes droop control effects after a disturbance, without constructing a detailed dynamic model of the complete AC/DC system. Further, it facilitates the computation of updated references of the coordinated control.

B. COMBINED AC/MTDC POWER FLOW: SOLUTION METHOD

In this study, the unified approach, similar to the method in [28], was adopted to develop a generalized C-PF algorithm to solve the combined AC/MTDC grid. Generic droop control was also implemented to determine the effects of various power balancing controls. The problem of more than one AC grid solution was dealt with by categorizing the interconnected AC grids into integrated and non-integrated AC grids; AC and DC grids are considered to be integrated and can be solved simultaneously if the slack node of the DC grid is linked to the AC grid. The non-integrated asynchronous AC grids can be solved separately, and their outputs are added into the integrated AC/DC grid solution in the C-PF algorithm. Further, the C-PF algorithm can also be incorporated into the existing AC power flow models.

The steady state model for the combined AC/DC power flow calculation should consider the steady state behaviour of the active power versus the DC link voltage represented by the PV characteristics of the VSC station. The various DC voltage control methods implemented show that the PV characteristic can be a combination of more than one linear or nonlinear functions of the DC voltage. The expression for a single linear PV–droop characteristic of the *i*th VSC of the MTDC grid can be expressed as:

$$\Delta P_{DC,i} = K_{DC,i}\ (\Delta\ V_{DC,i}) \tag{1}$$

$$\Delta P_{DC,i} = P_{DC,REF\ i} - K_{DC,i}\ (V_{DC,i} - V_{DC,REF\ i}) \tag{2}$$

where,
$P_{DC,i}$ is the actual power at the DC node (node *i*) of the VSC station,
$P_{DC,REF\ i}$ is the desired reference power,
$K_{DC,i}$ is the droop gain of the DC droop voltage controller,
$V_{DC,i}$ is the actual DC link voltage at the VSC station,
$V_{DC,REF\ i}$ is the reference DC voltage, which is normally set as the rated DC link voltage at the VSC station.

The most generic tri-band control, which is shown in Fig. 2(b), is implemented in the combined AC/DC power flow algorithm. This comprises three droop bands depending on the DC link voltage levels, namely upper band, normal band, and lower band. The upper band is the region between $V_{DC,MAX}$ and $V_{DC,HIGH}$, the normal band region is between $V_{DC,HIGH}$ and $V_{DC,LOW}$, and the lower band region is between $V_{DC,LOW}$ and $V_{DC,MIN}$.

$V_{DC,MAX}$ and $V_{DC,MIN}$ are usually set to ±5% of the reference DC link voltage ($V_{DC,REF}$), whereas $V_{DC,HIGH}$ and $V_{DC,LOW}$ can be set to ±2% of $V_{DC,REF}$. Thus, the generic form of the tri-band (non-linear PV–droop) characteristics of the *i*th VSC station of the MTDC grid is expressed as:

$P_{DC,i}\ (V_{DC,i}) =$

This article has been accepted for publication in a future issue of this journal, but has not been fully edited. Content may change prior to final publication. Citation information: DOI 10.1109/ACCESS.2019.2944718, IEEE Access

$$P_{DC,REF\,i} - K_{DC1,i}\,(V_{DC,i} - V_{DC,HIGH\,i}) \quad \text{if } V_{DC,HIGH\,i} < V_{DC,\,i} < V_{DC,MAX}$$

$$P_{DC,REF\,i} - K_{DC2,i}\,(V_{DC,i} - V_{DC,HIGH\,i}) \quad \text{if } V_{DC,LOW\,i} < V_{DC,\,i} < V_{DC,HIGH\,i}$$

$$P_{DC,REF\,i} - K_{DC3,i}\,(V_{DC,i} - V_{DC,LOW\,i}) - K_{DC2,i}\,(\Delta V_{K2,i}) \quad \text{if } V_{DC,MIN} < V_{DC,\,i} < V_{DC,LOW\,i}$$

where,

$P_{DC,i}$ is the actual power at the DC side of the VSC station,

$P_{DC,REF\,i}$ is the desired reference power,

$V_{DC,i}$ is the actual DC link voltage at the VSC station,

$K_{DC1,i}$, $K_{DC2,i}$ and $K_{DC3,i}$ are the droop gains of the DC droop voltage controller for the normal, upper, and lower bands, respectively,

$V_{DC,HIGH\ i}$ and $V_{DC,LOW\ i}$ are the upper and lower DC link voltages for the normal band operation references of the *i*th VSC station,

$\Delta V_{K2,I} = V_{DC,HIGH\,i} - V_{DC,LOW\,i}$,

$V_{DC,MAX}$ is the upper limit of the DC link voltage, which is mainly defined by the insulation requirements of the switching components.

$V_{DC,MIN}$ is the lower limit. The DC link should not be discharged below its lower limit to maintain normal operation of the VSC station.

The implementation of almost all the other control configurations is also possible by varying the value of the droop gains. For example, by setting the normal band droop gain K_{DC2} to zero, an infinite (very high) droop gain for the upper band (K_{DC1}) and the lower band (K_{DC3}) will yield DC voltage margin control, whereas setting all the three band droop gains equal will result in a simple linear DC voltage droop mode of distributed control. In dynamic simulations, a proportional–integral (PI) controller is used to implement constant DC voltage control; however, it can be theoretically represented with an infinite (very high) value of droop gain.

V. OPTIMIZED POWER FLOW CONTROL IN AC/MTDC GRIDS – TERTIARY CONTROL

Tertiary control is the upper layer control that enables security constrained economic dispatch (SCED) by providing a secure and operational plan for the integrated AC/MTDC grid. This takes the technical aspects into consideration and includes their economic constraints according to the given objective function. It provides optimal and secure references to VSC stations and AC generators. The time horizon for SCED can be in the range of 20–60 min. The references for the VSC stations include optimal power and DC voltage references and optimal reactive power or AC voltage references. In addition, tertiary control may reduce and increase the DC voltage limits for the normal operating band of tri-band voltage control.

Tertiary control involves optimal power flow (OPF) algorithms to obtain the optimal operating references according to the given objective function. Conventional OPF is essential for power system operation and is mainly applied to minimize the operating cost and losses. However, in the case of an integrated AC/MTDC grid, the security of the power system is equally as important as cost and loss minimization owing to the fast-acting power electronic devices in the MTDC grid. This study proposes a combined OPF (C-OPF) that incorporates security of the power system and enables the achievement of an optimal operational plan along with sufficient security margin for secure operation of the integrated system under N-1 reliability criterion. Further, power generation in the MTDC grid is mainly from OWFs; thus, tertiary control should also include stochastic wind forecasts as well as load forecasts for the AC grid.

A C-OPF of AC/DC grid is required to evaluate the potential effects of the MTDC grid on the steady state operation of the integrated AC/DC grid. It is essential to evaluate the benefit of the MTDC grid during the planning process as well as the optimal operation of the combined grid. The conventional AC OPF should be extended to include MTDC grid state variables and power flow equations; the formulation of the C-OPF for the combined AC/DC grids and the iterative process for security analysis based on C-OPF are described below.

A. COMBINED AC/MTDC OPTIMAL POWER FLOW: PROBLEM STATEMENT

The classical AC OPF can be written as a minimization of a general objective function $f(x)$, with equality constraints $g(x)$ and inequality constraints $h(x)$. The complete optimization case can be written as:

$$min_x\, f(x) \tag{4}$$

$$g(x) = 0 \tag{5}$$

$$h(x) \le 0 \tag{6}$$

$$x_{i\,min} \le x_i \le x_{i\,max} \tag{7}$$

where x is the optimization vector containing state and control variables. The state variables denoted by z determine the state of the system and comprise AC grid node angles and AC/DC grid node voltage magnitudes as given in (8), where δ_i and V_i are the angles and voltages at each AC bus node, respectively and $V_{DC,j}$ are the DC grid nodal voltages.

The control variables denoted by u include the active and reactive power injections from the generators and the VSC converters as given in (9), where P_{Gi} and Q_{Gi} are the power injections from the AC generators, $P_{VSC,\,j}$ and $Q_{VSC,\,j}$ are the AC side active and reactive power injection of the VSC, respectively and $I_{DC,\,j}$ are the DC branch currents.

The set of control variables may include the ratios and phase angles of tap changers or phase shifters or any other controlling device in the system; however, these were not taken into account in this study. If the AC grid comprises M nodes and the DC grid has N nodes, then $1 \le i \le M$ and $1 \le j \le N$. Equation (10) describes the complete optimization vector.

This article has been accepted for publication in a future issue of this journal, but has not been fully edited. Content may change prior to final publication. Citation information: DOI 10.1109/ACCESS.2019.2944718, IEEE Access

$$z = [\ \delta_i\ ,\ V_i\ ,\ V_{DC,j}\ ]^T \tag{8}$$

$$u = [P_{Gi}\ ,\ P_{VSC,j}\ ,\ Q_{Gi}\ ,\ Q_{VSC,j}\ ,\ I_{DC,j}\ ]^T \tag{9}$$

$$x = [\delta_i\ ,\ V_i\ ,\ P_{Gi}\ ,\ P_{VSC,j}\ ,\ Q_{Gi}\ ,\ Q_{VSC,j}\ ,\ I_{DC,j}\ ]^T \tag{10}$$

B. COMBINED AC/MTDC OPTIMAL POWER FLOW: SOLUTION METHOD

The optimization problem can be solved using simplified linear or full non-linear formulation. The solution of the simplified formulation is much faster and reduces computation resources; however, the accuracy of the results may be significantly low and it may not be able to determine the reactive power and voltage levels or losses in the system. The choice of the optimization solver mainly depends on the formulation of the problem, and a specific solver may be required to solve non-linear and non-convex problems, such as the interior-point method implemented in [30] and the second order cone method proposed in [43].

In this study, a non-linear formulation of the C-OPF is proposed to obtain accurate references from tertiary control for optimal scheduling. The algorithm was implemented in MATLAB using *fmincon*, which is an optimization toolbox function that finds the minimum constrained nonlinear multivariable functions. The non-linear formulation of the C-OPF problem in this study was solved using the *fmincon* solver in combination with the interior-point algorithm. However, a global optimal solution cannot be guaranteed when *fmincon* is used, that is, a better solution may exist. The objective here is to formulate an optimization algorithm for the combined AC/DC grids; global optimization is very time consuming, and is beyond the scope of this study. A more stable optimum can be ensured, if required, by running *fmincon* several times with different initial conditions.

C. PROPOSED SECURITY FOR COMBINED AC/MTDC GRIDS: PROPOSED METHOD

Security assessment is an iterative process, as shown in Fig. 4. The basic steps for the iterative process are described below.

1) Develop a base case scenario with forecast OWF connected through the MTDC grid, generation and load demand of the combined AC/DC system.

2) Solve the C-OPF for the base case to obtain the optimal operational plan of the system using the algorithm of any defined objective, that is cost minimization, loss minimization, etc.

3) Prepare a list of feasible contingencies and apply them one by one. Set counter i=1. Here, feasible contingencies refer to those contingencies that do not result in isolation of any generator or load in the combined AC/DC system.

4) Solve the C-PF and check if the optimal operating condition is secure for contingency i. If it is secure, then increase the counter; otherwise, apply some decision-based rules to mitigate the contingency. For example, if the voltages at some buses are below the minimum limit, then add reactive compensation using PV controlled converters.

Once all feasible contingencies have been applied, the optimal plan obtained will be secure and can be implemented for SCED in tertiary control. However, the limitation of this process is that the cost of security cannot be determined.

VI. TEST CASE

The original IEEE 14 bus network represents a portion of the American Power System (in the Midwestern US). This system comprises 14 buses, 20 branches, 5 generators, and 11 loads. Data for this system was obtained from MATPOWER [44]. Three generators act as synchronous condensers to provide reactive compensation. The system is also equipped with two winding and three winding transformers. The original 14 bus system was modified by adding a portion of an MTDC grid, and was employed in this study to perform combined AC/MTDC power flow analysis using the proposed combined algorithm. The first seven AC branches of the IEEE 14 bus AC network were converted to DC branches connected to the AC grid via VSC stations to model a DC grid with a five-terminal MTDC system. This produces a test case system of an integrated AC/MTDC 14 bus network, as shown in Fig. 5. The values of the line impedances and loads of the AC network are the same as in the original IEEE 14 bus data (refer to Appendix A for input data of the modified IEEE 14 bus network). Two synchronous condensers were modified to synchronous generators. One synchronous generator and two transformers were left out. The loads were modelled as constant PQ loads and the generator at *node 8* was modelled as a PV node with *node 1* as the slack bus. The OWF at *node 2* and the asynchronous AC grid at *node 3* were modelled as slack buses. Details of the operating modes of the converter and their ratings are presented in Table I.

In the five-terminal MTDC system, VSC1 (slack node) regulates the DC link voltage at ±200 kV (1pu). Other VSC converters were set to control the power measured at the PCC of each converter station. PVSC2 and PVSC3 inject 200 MW and 50 MW into the MTDC grid, respectively, whereas PVSC4 and PVSC5 were set to supply 60 MW to the AC system. The lengths of the DC grid cables were assumed to be l12 = 120 km, l15 = 70 km, l25 = 100 km, l24 = 150 km, l23 = 150 km, l34 = 70 km, and l45 = 100 km.

A. GENERIC TRI-BAND DROOP CONTROL IMPLEMENTATION

The detailed implementation of the generic tri-band droop control in the combinational power flow algorithm presented in section IV was applied to two cases of droop control under different scenarios: Case (a) without coordinated control; and Case (b) with rescheduling from coordinated control. The

This article has been accepted for publication in a future issue of this journal, but has not been fully edited. Content may change prior to final publication. Citation information: DOI 10.1109/ACCESS.2019.2944718, IEEE Access

detailed operating condition of the AC grid and VSC stations is presented in Table II. The test case system was assumed to be over dependent on OWF power generation to highlight its influence. Three scenarios were simulated using the power variation and outage of the OWF. In the first scenario, the OWF produces very high power of 200 MW. In the second scenario, an outage occurs in the OWF, whereas in the third scenario, the OWF produces a nominal power of 80 MW. The droop gains (K_{DC}) of all three droop bands were set to 20 in Case (a) and (b) such that the PV–droop characteristics of the DC droop control is linear. The values of the DC voltage for the droop bands are listed in Table II.

1) TRIBAND DROOP CONTROL WITHOUT COORDINATED CONTROL-CASE (A)

The PV–droop characteristic of *VSC4* and *VSC*5 are shown in Fig. 6 (a) and Fig. 6 (b), respectively, with three different linear droop lines in the three bands according to the specified voltage levels. The DC node voltage and active power of *VSC4* and *VSC5* in the three scenarios are shown in Fig. 6 (c) and Fig. 6 (d), represented as OP_0, OP_1, and OP_2 for the first scenario, second scenario, and third scenario, respectively. In the first scenario, the voltage and power at the DC *node 4* and *node 5* are high owing to very high power penetration from the OWF into the MTDC grid; thus, both VSC stations can be seen to operate in the upper bands of their respective PV–droop characteristics. However, once an outage occurs in the OWF in the second scenario, the voltage and power in both VSC stations drop; *VSC4* starts to operate in the lower droop band and *VSC5* operation goes into the normal droop band of the PV–droop characteristics, as shown by OP_1 in Fig. 6 (a) and Fig. 6 (b), respectively. In the third scenario, the OWF produces nominal power, and as expected, the voltage and power of both VSC stations return to their nominal values and operate in the normal droop band of the PV characteristics, as shown by OP_2 in Fig. 6 (a) and Fig. 6 (b).

2) TRIBAND DROOP CONTROL WITH COORDINATED CONTROL-CASE (B)

Fig. 7 shows the voltage and power of VSC4 and VSC5 under linear droop control with rescheduling from coordinated control during the second scenario, i.e. OWF outage. It can be observed from Fig. 7 (a) and Fig. 7 (b) that the voltage profiles of both VSC stations can be maintained in the upper and normal bands through power compensation using coordinated control.

B. COMPARISON OF OPTIMAL PLAN WITH AND WITHOUT SECURITY ASSESSMENT

A case study was carried out on the modified IEEE test network to demonstrate the importance of considering security constraints in the optimization of tertiary control. The test network was solved for minimized cost of generation with 50 MW of generation from the OWF. A feasible optimal plan obtained from the C-OPF can be used for operational planning at the tertiary control level to provide optimal references to the generator units of the AC grid and converter stations of the DC grid presented in Table IV.

Further, security assessment was performed against all feasible contingencies without carrying out any corrective action to the optimal plan. Fig. 8 shows the voltage profiles of six critical buses under six credible contingencies. It can be observed that the voltages at the critical buses fall well below the ±6% voltage regulation limits (assumed for this test network) during four contingencies.

Accordingly, the decision-based rules are defined such that if there is a drop in the voltage, then the set point of the PV-controlled VSC stations can be increased to provide reactive power compensation. A secure optimal reference plan for tertiary control is presented in Table V when the complete iterative process of security assessments proposed in section V(C) is applied with the required corrective actions. Fig. 9 shows the voltage profiles at the same buses under the same contingencies. It can be clearly observed that the voltage profiles at all the critical buses can be maintained within the prescribed ±6% voltage regulation limits by increasing the reactive power from VSC4 and VSC5 during the contingencies.

The cost of security was determined by comparing the cost function values before and after security assessments. It can be observed that the cost of security is almost negligible in this case as optimization was performed taking only the active power cost into account, which in this case accounts for only losses due to reactive power flow. The cost of security is estimated to be approximately 10 ¢/h in addition to the actual generating cost.

VII. CONCLUSION

The problem of determining a robust and reliable control strategy for operating combined AC/MTDC grids is complex, with many different aspects. This paper highlights the main challenges encountered in achieving such a robust strategy and presents an approach to tackle some of the challenges. The main aspects of primary, secondary, and tertiary control layers were presented. A hierarchical control structure for secure and optimal operation of integrated AC/MTDC grids that incorporates VSC control modes in power flow and nonlinear AC optimal power flow was presented. It was observed that the security of the combined AC/DC grid operation is as important as its economic operation. The proposed method was demonstrated using a modified version of a 14-bus test case system. A comparison of the optimal plan with and without security assessment demonstrated the robustness of the planning process. The results of this study highlight the importance of taking the security criterion into consideration in the modelling framework. Furthermore, the security assessments performed during tertiary control provide optimal references that are

secure under the given set of credible contingencies for generation dispatch. Future work will focus on simulation of the proposed method on test cases with many nodes and multiple MTDC grids attached to an AC system.

REFERENCES

[1] S. S. Torbaghan, M. Gibescu, B. G. Rawn, and M. van der Meijden, "A Market-Based Transmission Planning for HVDC Grid-Case Study of the North Sea," *IEEE Trans. Power Syst.*, vol. 30, no. 2, pp. 1–11, 2014.

[2] S. Cole and P. Martinot, "Study of the Benefits of a Meshed Offshore Grid in Northern Seas Region," *Eur. Comm.*, p. 102, 2014.

[3] F. D. Bianchi and O. Gomis-Bellmunt, "Droop Control Design for Multi-terminal VSC-HVDC Grids based on LMI Optimization," *IEEE Conf. Decis. Control Eur. Control Conf.*, pp. 4823–4828, Dec. 2011.

[4] C. Barker and R. Whitehouse, "Autonomous Converter Control in a Multi-terminal HVDC System," *Int. Conf. AC DC Power Transm.*, pp. 1–5, 2010.

[5] K. Rouzbehi, A. Miranian, J. I. Candela, A. Luna, and P. Rodriguez, "A generalized voltage droop strategy for control of multiterminal DC grids," *IEEE Trans. Ind. Appl.*, vol. 51, no. 1, pp. 607–618, 2015.

[6] K. Rouzbehi, J. Zhu, W. Zhang, G. B. Gharehpetian, A. Luna, and P. Rodriguez, "Generalized voltage droop control with inertia mimicry capability-step towards automation of multi-terminal HVDC grids," *2015 Int. Conf. Renew. Energy Res. Appl. ICRERA 2015*, vol. 5, pp. 1556–1561, 2015.

[7] W. Wang, M. Barnes, and O. Marjanovic, "Droop Control Modelling and Analysis of Multi-terminal HVDC for Offshore Wind Farms," *10th IET Int. Conf. AC DC Power Transm. (ACDC 2012)*, pp. 1–6, 2012.

[8] C. Dierckxsens, K. Srivastava, M. Reza, S. Cole, J. Beerten, and R. Belmans, "A Distributed DC Voltage Control Method for VSC MTDC Systems," *Electr. Power Syst. Res.*, vol. 82, no. 1, pp. 54–58, 2012.

[9] T. K. Vrana, L. Zeni, and O. B. Fosso, "Active Power Control with Undead-band Voltage & Frequency Droop Applied to a Meshed DC Grid Test System," in *Energy Conference and Exhibition (ENERGYCON), IEEE International*, 2012, pp. 612–616.

[10] T. K. Vrana, J. Beerten, R. Belmans, and O. B. Fosso, "A Classification of DC Node Voltage Control Methods for HVDC Grids," *Electr. Power Syst. Res.*, vol. 103, pp. 137–144, 2013.

[11] F. Thams, R. Eriksson, and M. Molinas, "Interaction of Droop Control Structures and Its Inherent Effect on the Power Transfer Limits in Multiterminal VSC-HVDC," *IEEE Trans. Power Deliv.*, vol. 32, no. 1, pp. 182–192, 2017.

[12] G. Stamatiou and M. Bongiorno, "Power-dependent droop-based control strategy for multi-terminal HVDC transmission grids," *IET Gener. Transm. Distrib.*, pp. 1–17, 2016.

[13] P. Rodriguez and K. Rouzbehi, "Multi-terminal DC grids: challenges and prospects," *J. Mod. Power Syst. Clean Energy*, vol. 5, no. 4, pp. 515–523, 2017.

[14] F. Azma and H. Rajabi Mashhadi, "DC voltage control and power-sharing of multi-terminal DC grids based on optimal DC power flow and voltage droop strategy," *Iran. J. Electr. Electron. Eng.*, vol. 11, no. 2, pp. 137–144, 2015.

[15] E. Veilleux and B. Ooi, "Power Flow Analysis in Multi-Terminal HVDC Grid," in *Power Systems Conference and Exposition (PSCE)*, 2011, pp. 1–7.

[16] T. M. Haileselassie and K. Uhlen, "Power Flow Analysis of Multi-terminal HVDC Networks," *2011 IEEE Trondheim PowerTech*, no. 4, pp. 1–6, Jun. 2011.

[17] R. Pinto, S. Rodrigues, E. Wiggelinkhuizen, R. Scherrer, P. Bauer, and J. Pierik, "Operation and Power Flow Control of Multi-Terminal DC Networks for Grid Integration of Offshore Wind Farms Using Genetic Algorithms," *Energies*, vol. 6, no. 1, pp. 1–26, Dec. 2012.

[18] F. Gonzalez-Longatt, J. Roldan, and C. A. Charalambous, "Power Flow Solution on Multi-Terminal HVDC Systems : Supergrid Case," in *International Conference on Renewable Energies and Power Quality (ICREPQ'12)*, 2012.

[19] Y. Liu, T. C. Green, J. Wu, K. Rouzbehi, A. Raza, and D. Xu, "A New Droop Coefficient Design Method for Accurate Power-Sharing in VSC-MTDC Systems," *IEEE Access*, vol. 7, pp. 47605–47614, 2019.

[20] J. Beerten, D. Van Hertem, and R. Belmans, "VSC MTDC Systems with a Distributed DC Voltage Control – A Power Flow Approach," in *IEEE Trondheim PowerTech*, 2011, pp. 1–6.

[21] M. Baradar, M. Ghandhari, and D. Van Hertem, "The Modeling Multi-terminal VSC-HVDC in Power Flow Calculation using Unified Methodology," *2011 2nd IEEE PES Int. Conf. Exhib. Innov. Smart Grid Technol.*, pp. 1–6, Dec. 2011.

[22] R. Z. Chai, B. H. Zhang, Z. Q. Bo, and J. M. Dou, "A Generalized Unified Power Flow Algorithm for AC / DC Networks Containing VSC-Based Multi-terminal DC Grid," in *International Conference on Power System Technology (POWERCON 2014)*, 2014, pp. 20–22.

[23] F. Gonzalez-Longatt, J. M. Roldan, E. S. De Ingenieros, and C. A. Charalambous, "Solution of AC / DC Power Flow on a Multi-Terminal HVDC System : Illustrative Case Supergrid Phase I," in *47th International Universities Power Engineering Conference*, 2012, pp. 1–7.

[24] E. Rakhshani, D. Remon, A. M. Cantarellas, K. Rouzbehi, and P. Rodriguez, "Integration of renewable generation for frequency support of HVDC/AC interconnected systems under power market scenario," *IEEE Power Energy Soc. Gen. Meet.*, vol. 2014-October, no. October, 2014.

[25] A. Raza *et al.*, "Power Dispatch and Voltage Control in Multiterminal HVDC Systems: A Flexible Approach," *IEEE Access*, vol. 5, pp. 24608–24616, 2017.

[26] W. Wang and M. Barnes, "Power Flow Algorithms for Multi-terminal VSC-HVDC with Droop Control," *IEEE Trans. Power Syst.*, vol. 29, no. 4, pp. 1721–1730, 2014.

[27] J. Beerten, S. Cole, and R. Belmans, "Generalized Steady-State VSC MTDC Model for Sequential AC / DC Power Flow Algorithms," *IEEE Trans. POWER Syst.*, vol. 27, no. 2, pp. 821–829, 2012.

[28] M. Baradar and M. Ghandhari, "A Multi-Option Uni fi ed Power Flow Approach for Hybrid AC /DC Grids Incorporating Multi-terminal VSC-HVDC," *IEEE Trans. POWER Syst.*, vol. 28, no. 3, pp. 2376–2383, 2013.

[29] R. Wiget and G. Andersson, "Optimal Power Flow for Combined AC and Multi-terminal HVDC Grids based on VSC Converters," *2012 IEEE Power Energy Soc. Gen. Meet.*, pp. 1–8, Jul. 2012.

[30] J. Rimez, "A Combined AC/DC Optimal Power Flow Algorithm for Meshed AC and DC Networks Linked by VSC Converters," *Electr. Power Syst. Res.*, vol. 20, no. 2, pp. 1–6, 2009.

[31] M. Baradar and M. R. Hesamzadeh, "Modelling of Multi-Terminal HVDC Systems in Optimal Power Flow Formulation," *IEEE Electr. Power Energy Conf.*, pp. 170–175, 2012.

[32] M. Aragüés-Peñalba, J. Beerten, J. Rimez, D. Van Hertem, and O. Gomis-bellmunt, "Optimal Power Flow Tool for Hybrid AC/DC Systems," in *11th IET Int. Conf. AC DC Power Transm.*, 2015.

[33] K. Meng *et al.*, "Hierarchical SCOPF Considering Wind Energy Integration Through Multiterminal VSC-HVDC Grids," *IEEE Trans. Power Syst.*, vol. 32, no. 6, pp. 4211–4221, 2017.

[34] A. Raza *et al.*, "Optimal Power Flow and Unified Control Strategy for Multi-Terminal HVDC Systems," *IEEE Access*, vol. 7, pp. 1–1, 2019.

[35] G. Roger Wiget, Emil Iggland and O. Andersson, "Security Constrained Optimal Power Flow for HVAC and HVDC Grids," *PowerTech*, 2015.

[36] S. Chatzivasileiadis, "Security Constrained OPF Incorporating Corrective Control of HVDC," in *Power Systems Computation Conference (PSCC)*, 2014.

[37] F. Akhter, D. E. Macpherson, and G. P. Harrison, "Enhanced Multi-terminal HVDC Grid Management for Reliable AC

Network Integration," *7th IET Int. Conf. Power Electron. Mach. Drives (PEMD 2014)*, pp. 0495–0495, 2014.

[38] X. Li, L. Guo, C. Hong, Y. Zhang, Y. W. Li, and C. Wang, "Hierarchical Control of Multiterminal DC Grids for Large-Scale Renewable Energy Integration," *IEEE Trans. Sustain. Energy*, vol. 9, no. 3, pp. 1448–1457, 2018.

[39] M. Aragüés-Peñalba, A. Egea-Àlvarez, O. Gomis-Bellmunt, and A. Sumper, "Optimum Voltage Control for Loss Minimization in HVDC Multi-terminal Transmission Systems for Large Offshore Wind Farms," *Electr. Power Syst. Res.*, vol. 89, pp. 54–63, Aug. 2012.

[40] A. Egea-Alvarez, J. Beerten, D. Van Hertem, and O. Gomis-Bellmunt, "Hierarchical power control of multiterminal HVDC grids," *Electr. Power Syst. Res.*, vol. 121, pp. 207–215, 2015.

[41] K. Rouzbehi, A. Miranian, J. I. Candela, A. Luna, and P. Rodriguez, "A hierarchical control structure for multi-terminal VSC-based HVDC grids with GVD characteristics," *Proc. 2013 Int. Conf. Renew. Energy Res. Appl. ICRERA 2013*, no. October, pp. 996–1001, 2013.

[42] CIGRE Working Group B4.52, "HVDC Grid Feasibility Study," 2013.

[43] M. Baradar, M. R. Hesamzadeh, and M. Ghandhari, "Second-order Cone Programming for Optimal Power Flow in VSC-Type AC-DC Grids," *IEEE Trans. Power Syst.*, vol. 28, no. 4, pp. 4282–4291, 2013.

[44] R. D. Zimmerman, C. E. Murillo Sánchez, and R. J. Thomas, "MATPOWER: Steady-State Operations, Planning, and Analysis Tools for Power Systems Research and Education," *Power Syst. IEEE Trans.*, vol. 26, no. 1, pp. 12–19, 2011.

This article has been accepted for publication in a future issue of this journal, but has not been fully edited. Content may change prior to final publication. Citation information: DOI 10.1109/ACCESS.2019.2944718, IEEE Access

List of figures

This article has been accepted for publication in a future issue of this journal, but has not been fully edited. Content may change prior to final publication. Citation information: DOI 10.1109/ACCESS.2019.2944718, IEEE Access

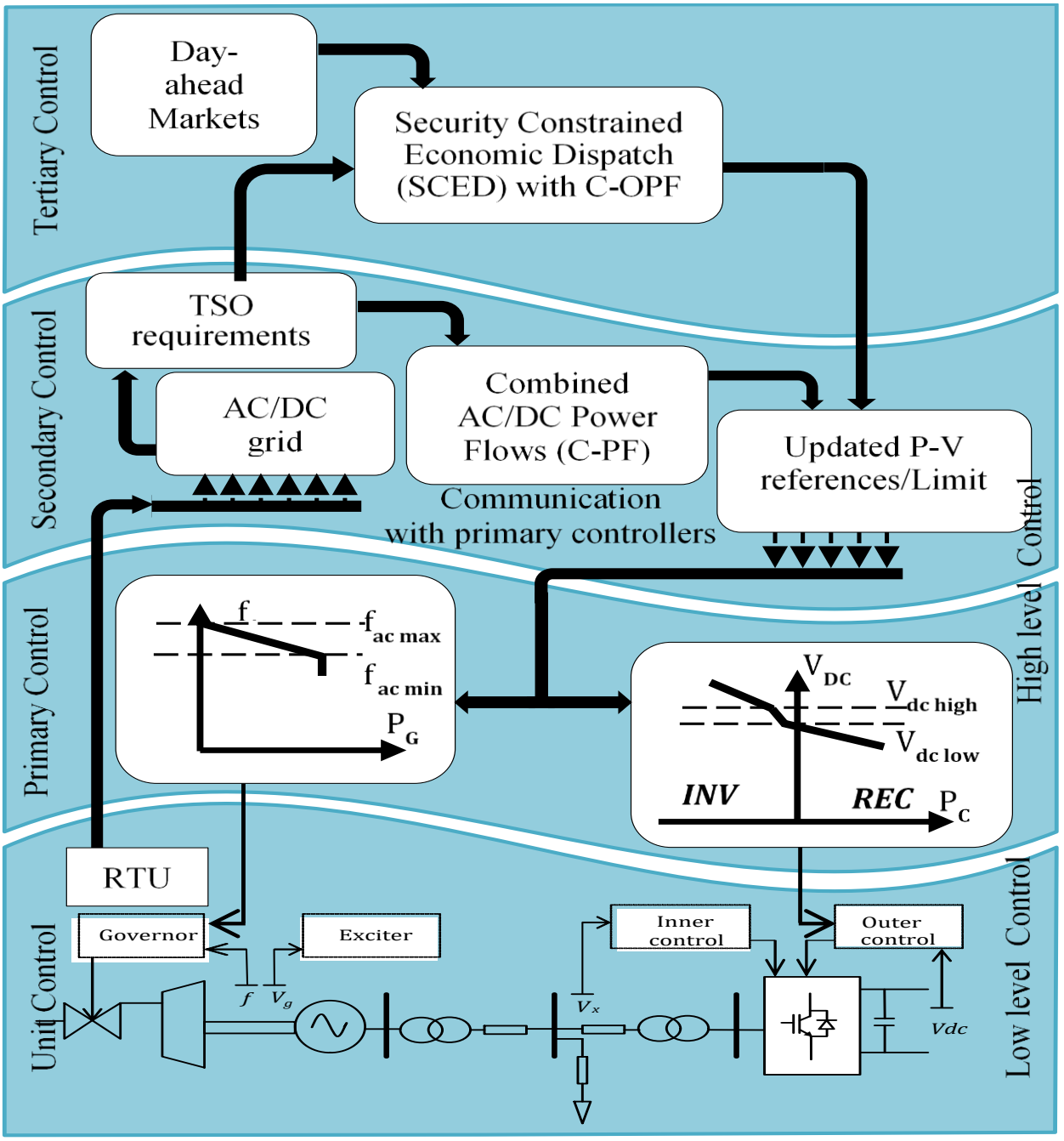

FIGURE 1

This article has been accepted for publication in a future issue of this journal, but has not been fully edited. Content may change prior to final publication. Citation information: DOI 10.1109/ACCESS.2019.2944718, IEEE Access

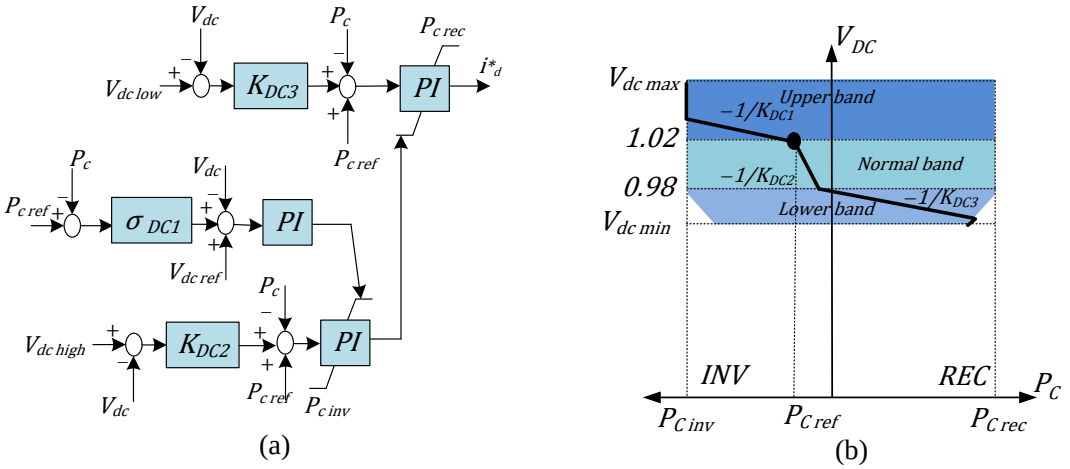

FIGURE 2

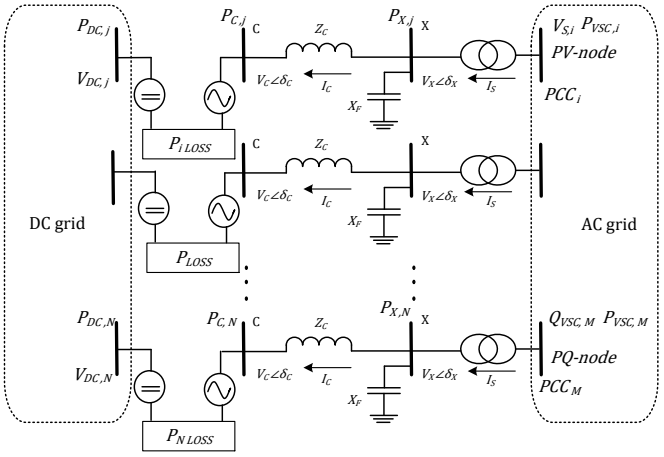

FIGURE 3

This article has been accepted for publication in a future issue of this journal, but has not been fully edited. Content may change prior to final publication. Citation information: DOI 10.1109/ACCESS.2019.2944718, IEEE Access

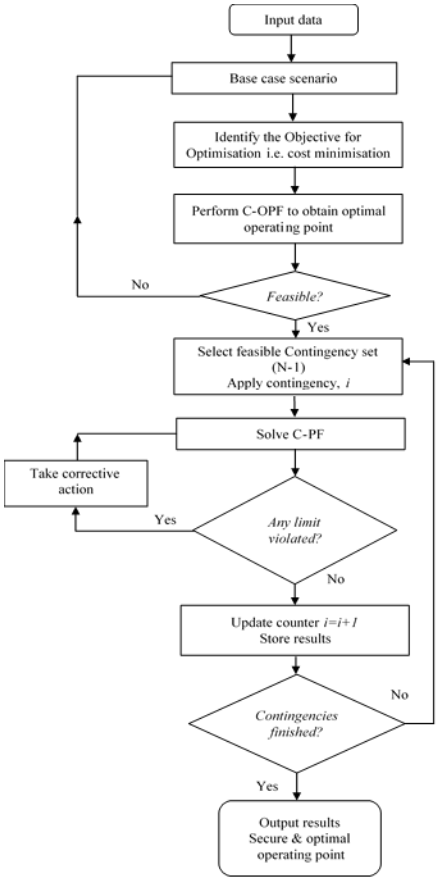

FIGURE 4

This article has been accepted for publication in a future issue of this journal, but has not been fully edited. Content may change prior to final publication. Citation information: DOI 10.1109/ACCESS.2019.2944718, IEEE Access

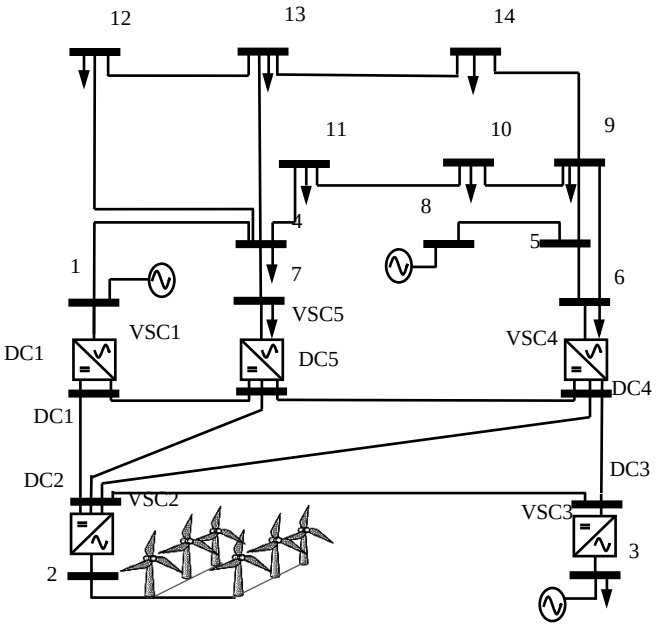

FIGURE 5

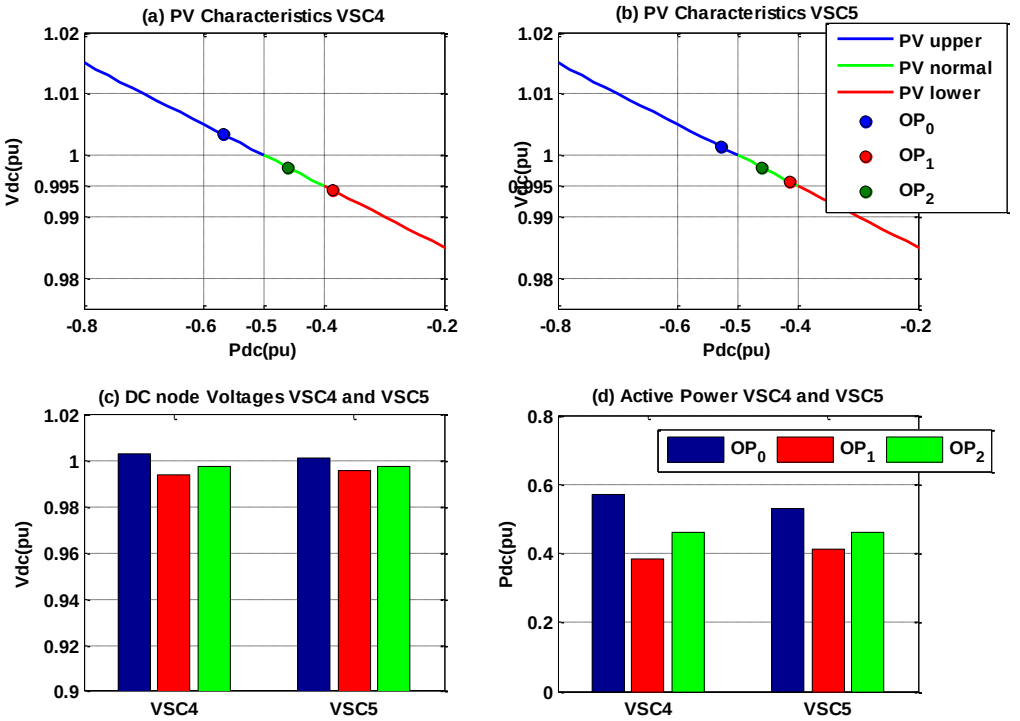

FIGURE 6

This article has been accepted for publication in a future issue of this journal, but has not been fully edited. Content may change prior to final publication. Citation information: DOI 10.1109/ACCESS.2019.2944718, IEEE Access

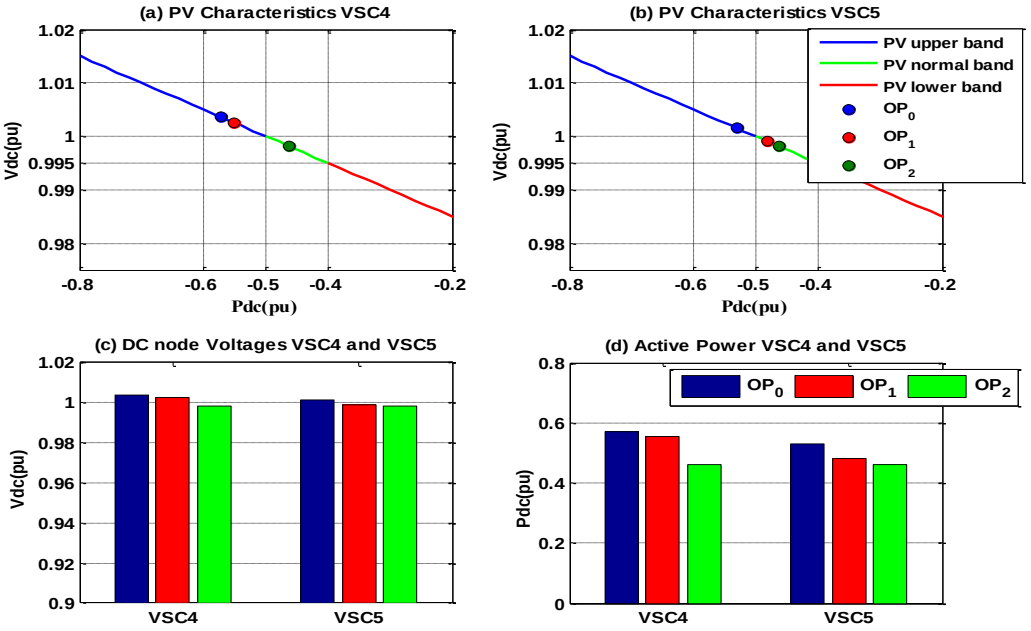

FIGURE 7

This article has been accepted for publication in a future issue of this journal, but has not been fully edited. Content may change prior to final publication. Citation information: DOI 10.1109/ACCESS.2019.2944718, IEEE Access

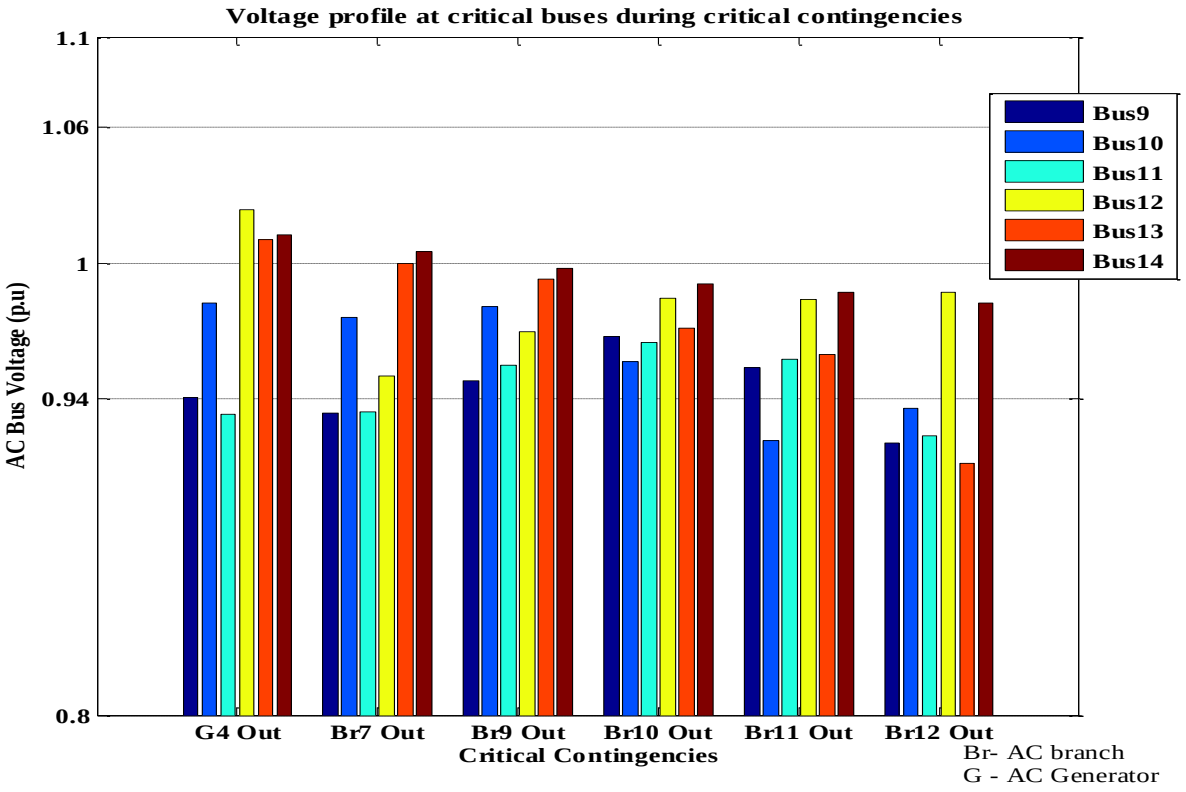

FIGURE 8

This article has been accepted for publication in a future issue of this journal, but has not been fully edited. Content may change prior to final publication. Citation information: DOI 10.1109/ACCESS.2019.2944718, IEEE Access

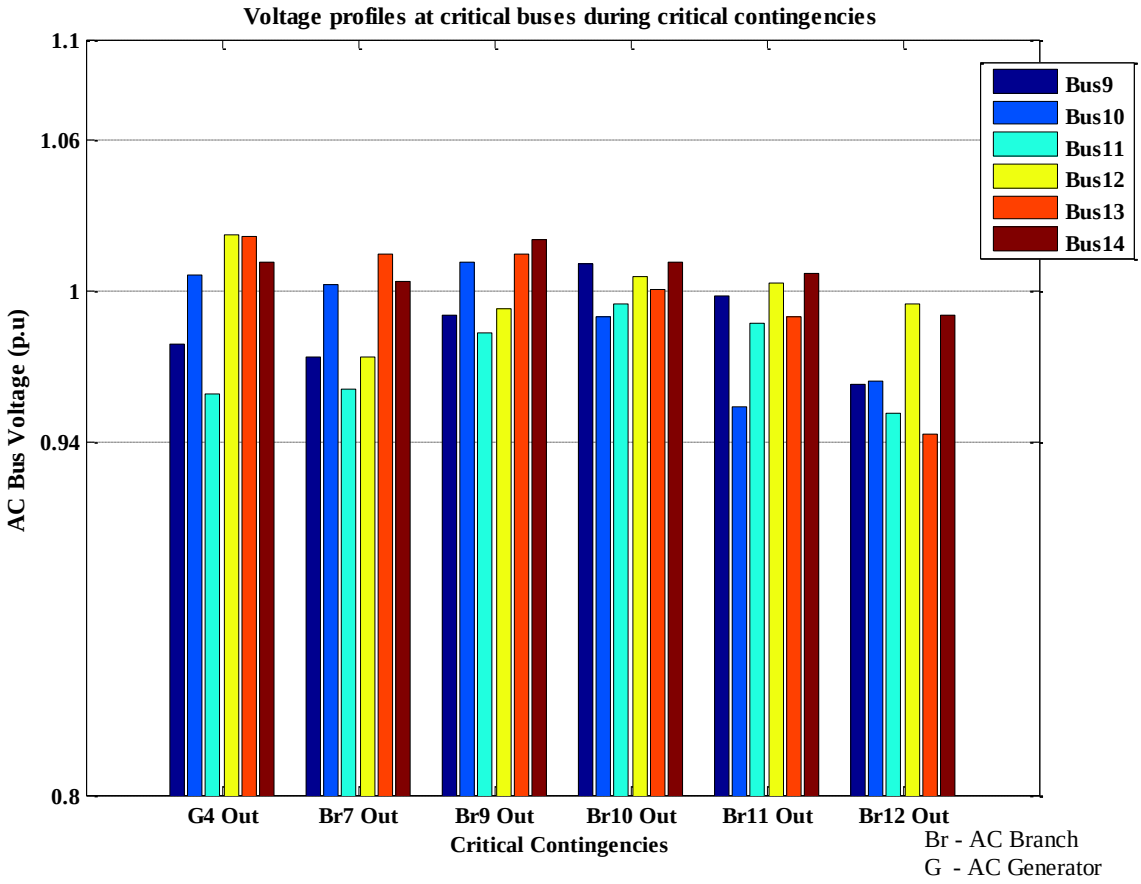

FIGURE 9

This article has been accepted for publication in a future issue of this journal, but has not been fully edited. Content may change prior to final publication. Citation information: DOI 10.1109/ACCESS.2019.2944718, IEEE Access

List of tables

This article has been accepted for publication in a future issue of this journal, but has not been fully edited. Content may change prior to final publication. Citation information: DOI 10.1109/ACCESS.2019.2944718, IEEE Access

TABLE I

VSC stations	***P_{VSC} (MW)***	***V_{DC} (kV)***	***VSC control***	***PCC Type***	***AC grid node***
VSC1	*slack*	±200	V_{DC}-control	PQ	Bus1
VSC2	-200	±200	P-control	PQ	Bus2
VSC3	-50	±200	P-control	PQ	Bus3
VSC4	60	±200	P-control	PV	Bus6
VSC5	60	±200	P-control	PV	Bus7

TABLE II

AC grid node	*Gen:*	*V_{AC}* (p.u)	*P_G* (MW)	*PCC* type	*VSC*	*P_{VSC}* (MW)	*VSC* control
Bus1	Gen1	1.06	*slack*	PQ	1	*slack*	V_{DC}-control
Bus2	OWF	1.045	200	PQ	2	-200	P-control
Bus3	Gen3	1.01	34.2	PQ	3	-10	P-control
Bus6	-	1.0	-	PV	4	50	PV-droop
Bus7	-	1.0	-	PV	5	50	PV-droop
Bus8	Gen8	1.02	35	-	-	-	-

TABLE III

VSC stations	*V_{MAX} (pu)*	*V_{HIGH} (pu)*	*V_{LOW} (pu)*	*V_{MIN} (pu)*
VSC4	1.02	1	0.995	0.98
VSC5	1.02	1	0.995	0.98

TABLE IV

AC bus	***Gen***	***V_{AC}* (pu)**	***P_G* (MW)**	***Q_G* (MVAr)**	***VSC***	***P_{VSC}* (MW)**	***Q_{VSC}* (MVAr)**	***V_{DC}* (pu)**
1	Gen1	1.025	16.71	9.74	1	22.09	6.89	1.00
2	OWF	1.06	50	-1.75	2	-50	1.75	1.0025
3	Gen3	1.06	49.82	11.91	3	-25	7.09	1.0017
6	-	1.034	-	-	4	30.10	15.47	1.0004
7	-	1.023	-	-	5	17.04	7.50	0.9995
8	Gen8	1.06	67.71	25.4	-	-	-	-

TABLE V

AC bus	***Gen***	***V_{AC}* (pu)**	***P_G* (MW)**	***Q_G* (MVAr)**	***VSC***	***P_{VSC}* (MW)**	***Q_{VSC}* (MVAr)**	***V_{DC}* (pu)**
1	Gen1	1.04	16.71	7.32	1	22.09	6.89	1.00
2	OWF	1.06	50	-1.75	2	-50	1.75	1.0025
3	Gen3	1.06	49.82	11.91	3	-25	7.09	1.0017
6	-	1.05	-	-	4	30.10	19.13	1.0004
7	-	1.05	-	-	5	17.04	11.75	0.9995
8	Gen8	1.06	67.71	19.46	-	-	-	-